

Effect of Spatial, Temporal, and Velocity Resolution on Doppler Tissue Image Derived Indices

JL Rojo-Álvarez¹, J Bermejo², AB Rodríguez-González¹, R Yotti²,
A Martínez-Fernández¹, MA García-Fernández², JC Antoranz³

¹Universidad Carlos III de Madrid, Leganés, Madrid, Spain

²Hospital General Universitario Gregorio Marañón, Madrid, Spain

³Universidad Nacional de Educación a Distancia, Madrid, Spain

Abstract

Many indices derived from color Doppler Tissue Imaging (DTI) are computed mathematically from the velocity fields provided by the ultrasound scanner. We developed a procedure for assessing the uncertainty that temporal, spatial, and velocity resolution causes on cardiovascular parameters derived from myocardial velocity. A first-order Taylor's series for the functional relationship between velocity and the cardiac index under study is proposed, and analytically solved by using the chain rule. Performance on myocardial acceleration, strain, and strain rate, was tested both on a simulation model (symbolic calculations) and on a clinical image example. Velocity and temporal resolutions were the most determinant on DTI-derived parameters, and increasing color-Doppler bit-depth from 5 to 7 bits reduced to less than 10% the uncertainty of all the analyzed indices. Taylor-based error bounds are a useful tool to assess the effect of resolution on quantitative cardiovascular indices derived from tissue velocity measurements.

1. Introduction

Doppler echocardiography has become the most useful noninvasive technique to assess cardiovascular function. Pulsed-wave and color-Doppler Tissue Imaging (DTI) modalities were developed during the last decade [1, 2]. Based on the modification of Doppler flow filters, DTI provides accurate measurements of the velocity of the myocardial walls.

Most useful cardiac indices derived from DTI raw velocity data require actually mathematical operations. Endocardial tracking [3], myocardial acceleration [4], myocardial strain and myocardial strain-rate [5, 6] have demonstrated to be extremely sensitive for detecting and quantifying subtle cardiovascular abnormalities previously undetectable non-invasively. Mathematical derivation

of color-Doppler velocity-data is strongly dependent on noise and artifacts [7], and indices numerically derived from these images are heavily influenced by the lack of signal ("black holes"). Scanner resolutions in time (sampling frequency), space (pixels/cm), and velocity (bit-depth of the color-Doppler processor), are additional sources of uncertainty. But surprisingly, the effect of image resolution on indices derived from measurements of velocity has not been yet specifically addressed. Our aim is to propose a general method suitable to determine the magnitude of error that the resolution of the image acquisition system induces on each cardiac index. For this purpose, an analytical framework is proposed, from which the maximal error related to current ultrasound scanner resolutions can be calculated, in order to define where further technological efforts should focus on.

The draw of the paper is as follows. In the next section, error bounds for myocardial acceleration, strain, and strain-rate, are derived analytically, based on a first-order Taylor's series. The simulation model used is then described. Simulations of tissue deformation during a cardiac cycle are used to measure the impact of spatial, temporal, and velocity resolutions on DTI indices. Error bounds are provided for a true example of DTI image. Finally, conclusions are summarized.

2. Error bounds

Myocardial acceleration, strain, and strain-rate, can be expressed through mathematical operations that transform the velocity fields. A simple first order Taylor's series expansion can approximate this operator by a linear expression, and then, how each simple operation involved affects the cardiac index can be assessed from the chain rule. This sensitivity analysis procedure has been widely used to study the effect of coefficient quantization in structures for digital filters [8].

Error bounds using Taylor's series. Be $v_t(s, t)$ a tissue 1D+t velocity field (M-mode) that is measured as a function of time t and distance s from the transducer. Be f a cardiac index that is obtained by functional operations on $v_t(s, t)$. By taking the first order Taylor's series expansion of f in a given point $(s, t, v_t(s, t))$, and for small increments of time (δt), space (δs), and velocity (δv_t), we can express changes δf as

$$\delta f \simeq \frac{\partial f}{\partial s} \cdot \delta s + \frac{\partial f}{\partial t} \cdot \delta t + \frac{\partial f}{\partial v_t} \cdot \delta v_t \quad (1)$$

This equation represents an approximation to the influence that small increments on velocity, space, and time, produces on the increments of cardiac index f . Given that velocity is expressed as a function of time and space, coefficients of $\delta s, \delta t, \delta v_t$, are indeed two-variable expressions.

Without loss of generality, we will use a temporal cardiac index defined by a (continuous and differentiable) time function $f = f(t)$ to analyze time-varying waveforms. To obtain an upper bound of the effect of each resolution, it is assumed that the total influence of each partial derivative in the right term of (1) is mainly due to its value at instant t . For a spatial domain S , we have

$$|\delta f(t)| \leq c_s(t)\delta s + c_t(t)\delta t + c_v(t)\delta v_t \quad (2)$$

where

$$c_v(t) = \int_S \left| \frac{\partial f(t)}{\partial v_t(s, t)} \right| ds \quad (3)$$

and $c_s(t), c_t(t)$ can be calculated in a similar way.

The main issue in this procedure is the calculation of $\frac{\partial f}{\partial v_t}$, the other partial derivatives being obtained directly by the chain rule as:

$$\frac{\partial f}{\partial s} = \frac{\partial f}{\partial v_t} \frac{\partial v_t}{\partial s} \quad (4)$$

$$\frac{\partial f}{\partial t} = \frac{\partial f}{\partial v_t} \frac{\partial v_t}{\partial t} \quad (5)$$

Spatial domain of integration S is just the straight line along the spatial dimension of the image. However, if this domain integration results in too relaxed error bounds, S can be conveniently reduced according to previous *a priori* knowledge of the operator and/or the image, as it will be shown in the applications. Note that (2) is a highly pessimistic bound, because all errors are assumed to take place in the same orientation.

DTI derived indices. Myocardial acceleration is a measurement of the changes in tissue velocity along the ultrasound streamline, and it is computed [4] as

$$a(s, t) = \frac{\partial v_t(s, t)}{\partial t} \quad (6)$$

Natural strain-rate accounts for the speed at which deformation of an object occurs, and, in the case of cardiac strain rate, it represents the rate at which a given location of the myocardial wall thickens and thins. It can be obtained using DTI [9] as

$$\dot{\varepsilon}(s, t) = \frac{v_t(s, t) - v_t(s - L, t)}{L} \quad (7)$$

where $\dot{\varepsilon}(s, t)$ is the relative amount of cardiac wall deformation between two locations separated by a distance L , usually $L = 1 \text{ cm}$. Strain accounts for the deformation of an object, normalized to its original shape. The total amount of cardiac strain can be obtained from DTI [9] by simply adding infinitesimal strain contributions,

$$\varepsilon(s, t) = \int_{t_0}^t \dot{\varepsilon}(s, \tau) d\tau \quad (8)$$

In M-mode, acceleration, strain rate, and strain of the myocardium are also 1D + t fields (i.e., images). For simplicity, each cardiac index is obtained at a single spatial location s_0 , providing a waveform of its temporal variation.

Partial derivatives of (6), (7), (8) with respect to $v_t(s, t)$ are given by:

$$\frac{\partial a(s, t)}{\partial v_t(s, t)} = \frac{\partial v_t(s, t)}{\partial t} \quad (9)$$

$$\frac{\partial \dot{\varepsilon}(s, t)}{\partial v_t(s, t)} = \frac{1}{L} \left(1 - \frac{\partial v_t(s - L, t)}{\partial t} \left(\frac{\partial v_t(s, t)}{\partial t} \right)^{-1} \right) \quad (10)$$

$$\frac{\partial \varepsilon(s, t)}{\partial v_t(s, t)} = \int_{t_0}^t \frac{\partial \dot{\varepsilon}(s, \tau)}{\partial v_t(s, \tau)} d\tau \quad (11)$$

3. Image model

A simple model of DTI during a full cardiac cycle was created from 6 individual components, each of which combined an exponential and a polynomial expression, as

$$v_t(s, t) = \left(\frac{s}{4} - 1 \right)^2 \sum_{i=1}^6 a_i \exp \left\{ - \frac{\left(\frac{t+t_i}{t_a} \right)^2}{2\sigma_i^2} \right\} \quad (12)$$

where $t_a = 0.05 \text{ s}$. The six gaussian components correspond to diastolic early filling ($i = 1, 2$), atrial contraction ($i = 3$), isovolumic contraction ($i = 4$), and (fast and slow) systolic contraction ($i = 5, 6$) (Fig. 1). Time 0 was defined at QRS onset. Constant parameter values a_i and t_i were adjusted based on the following constrains:

- Physiological values for myocardial velocity (systolic and diastolic E-wave and A-wave), acceleration, strain, and strain-rate [4, 5].

i	1	2	3	4	5	6
t_i	0.25	0.20	0.03	-0.01	-0.06	-0.15
a_i	-9	-2.75	-9.95	3	9	5
σ_i	0.50	0.50	0.20	0.09	0.40	0.80

Table 1. Constant parameter values used in the DTI model defined in (12).

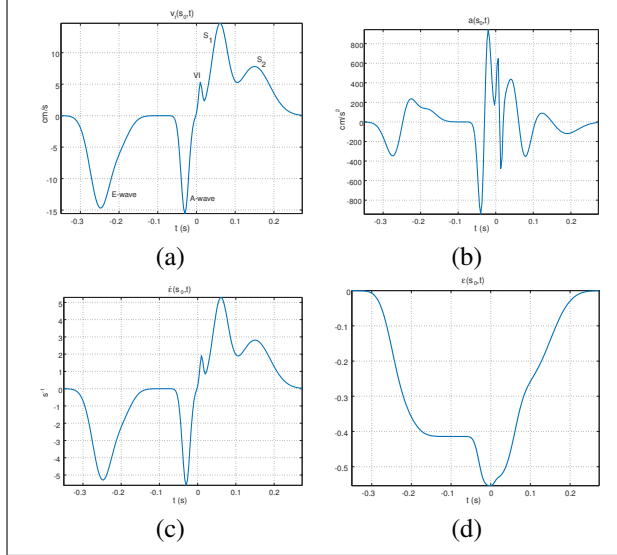


Figure 1. Waveforms from simulated color DTI M-mode, measured at $s_0 = 9$ cm: (a) velocity, (b) myocardial acceleration, (c) strain rate, and (d) strain.

- Time integrals of velocity and strain are zero at the end of the cardiac cycle.

These conditions were fulfilled by the set of values shown in Table 1. A symbolic velocity field $v_t(s, t)$ is obtained, suitable for computing analytically the exact derived indices and the exact theoretical error bounds. In the simulations, time interval was $(-0.350, 0.275)$ s, and spatial support was $(8, 10)$ cm far from the ultrasound transducer. The correspondent velocity image was simulated by sampling and quantifying the symbolic 2-D fields, with different sets of resolutions. Equations (9)-(11) were calculated on spatial location $s_0 = 9$ cm.

4. Results

Simulations. Discrete DTI images were simulated from the myocardial velocity model using the following two sets of resolutions:

- typical values of most ultrasound scanners, given by $\delta t = 1/200$ s, $\delta s = 1/20$ cm/pixel, and $\delta v_t = \frac{\text{upper} - \text{lower Nyquist limits}}{2^b}$ cm/s, where b is the number of bits (eg, for color scale limits of ± 10 cm/s and $b = 5$ bits, $\delta v_t = 20/32 = 0.625$ cm/s) [10, 11];

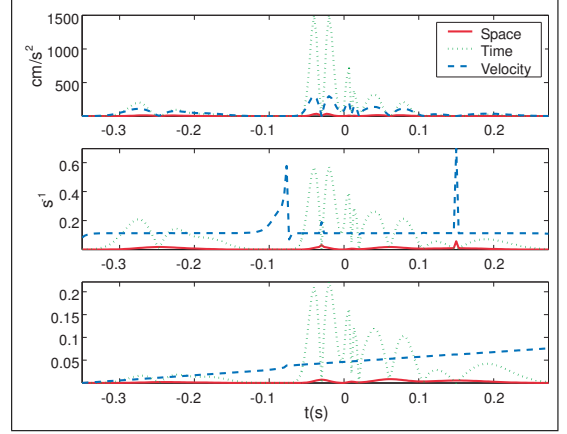


Figure 2. DTI error bounds obtained from the simulated myocardial velocity models, for nominal values of current ultrasound scanners. Error bounds for myocardial acceleration (up), strain rate (middle) and strain (down).

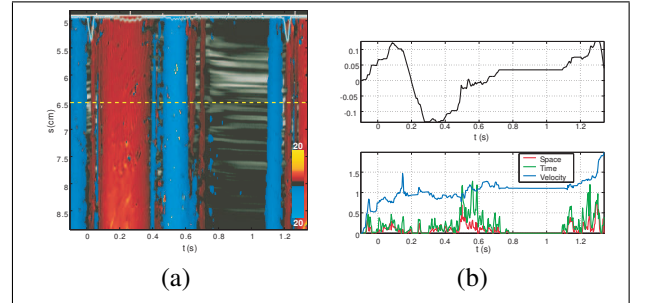


Figure 3. Example of resolution errors estimated from a clinical DTI image. (a) Color M-mode DTI of the mid-basal interventricular septum from a healthy volunteer. (b) Numerically estimated strain (up) and estimated Taylor error bounds for calculating total strain (down).

- improved resolution values, identified as the temporal, spatial, and velocity resolution values that reduced the maximum of the error bound below 10% of the peak of the cardiac index.

Acceleration, strain, and strain rate waveforms were calculated after a 3×3 median filtering, by discrete numerical derivation and/or integration of the velocity image.

Figure 2(a) shows the theoretical error bounds calculated analytically for scanner resolutions. Spatial resolution is appropriate for the three DTI indices. However, errors due to time and velocity resolutions are relevant for all of them. Velocity resolution is specially important to accurately measure peak myocardial acceleration values. Spikes in strain rate bounds of velocity are observed because (10) needs to be regularized by adding a small constant (0.1) to the denominator, in order to avoid dividing by zero. Noteworthy, strain error due to

	$1/\delta s$ (pix/cm)	$1/\delta t$ (Hz)	bits
Acceleration	22.1	4775	6.7
Strain Rate	6.2	306	5.4
Strain	9.0	1200	5.5
Resol. of current scanners	20	200	5

Table 2. Spatial, temporal, and velocity resolutions required to lower the theoretical error bound below 10% of the peak of each cardiac index.

velocity clearly increases over time, as a consequence of the integral operator involved in its calculation.

Table 2 presents the theoretical values required to decrease errors to 10% of the peak amplitude of each index. Velocity resolution for accurate acceleration measurements seems to be the most expensive (almost 7 bits per sample). An increase in sampling frequency is convenient for both acceleration and strain.

Application example. The image from a healthy volunteer is shown in Fig. 3(a). Scanner resolutions were $\delta_s = 1/20$ cm/pixel, $\delta_t = 1/200$ s, and 5 bits (equivalent to 1.25 cm/s). Error bounds were obtained for the raw image, with the same preprocessing as in previously modeled images. For the three indices, all the resolutions were shown to be poor. As an example, Fig. 3(b) presents the estimated error bounds for the estimated strain waveform. A typical error of current methods used for calculating myocardial strain from DTI curves can be observed: it does not return to baseline at the end of a cardiac cycle. In this example, velocity appears as the most important source of error.

5. Conclusions

A method for quantifying the impact of spatial, temporal, and velocity resolution on cardiac indices derived from DTI has been proposed, basing on a first order Taylor's series expansion of the functional that transforms the tissue velocity field into the numerical index. The efficacy of the method has been tested on a completely known simulation model. Though the error will be certainly dependent on the acquired image, the method can be applied to true images, still providing with the order of magnitude of the error. The statement of bounds for indices derived from color-Doppler flow images, as well as the use of the method in extensive image data bases, are the most immediate future applications.

Acknowledgements

This work has been partially supported by a research grant from the Fondo de Investigación Sanitaria (PI031220) of Instituto Carlos III, Madrid, Spain, and by a research grant from Sociedad Española de Cardiología, 2003. Dr R Yotti is supported by BEFI BF03-00031 of the Instituto Carlos III. Prof JC Antoranz is partially supported by SCIT 2000-2003 Contract Program of Comunidad de Madrid.

References

- [1] Isaza K, Thompson A, Etchevenot G, Cloez JL, Brembilla B, Pernot C. Doppler echocardiographic measurement of low velocity motion of the left ventricular posterior wall. *Am J Cardiol* 1989;64(1):66–75.
- [2] Fleming AD, Palka P, McDicken WN, Fenn LN, Sutherland GR. Verification of cardiac doppler tissue images using grey-scale m-mode images. *Ultrasound Med Biol* 1996; 22(5):573–81.
- [3] Pan C, Kühl M, Severin E, Franke A, Hanrath P. Tissue tracking allows rapid and accurate visual evaluation of left ventricular function. *Eur J Echocardiography* 2001;2:197–202.
- [4] Vogel M, Cheung M, Li J, Kristiansen S, Schmidt M, White P, Sorensen K, Redington A. Noninvasive assessment of left ventricular force-frequency relationships using tissue doppler-derived isovolumic acceleration. *Circulation* 2003; 107(12):1647–52.
- [5] Greenberg NL, Firstenberg MS, Castro PL, Main M, Travaglini A, Odabashian JA, Drinko JK, Rodriguez LL, Thomas JD, Garcia MJ. Doppler-derived myocardial systolic strain rate is a strong index of left ventricular contractility. *Circulation* 2002;105(1):99–105.
- [6] Smiseth OA, Ihlen H. Strain rate imaging: why do we need it? *J Am Coll Cardiol* 2003;42(9):1584–6.
- [7] Rao S, Richardson S, Simnetti J, Katz S, Caldeira M, Pandian N. Problems and pitfalls in the performance and interpretation of color doppler flow imaging: observations based on the influences of technical and physiological factors on the color doppler examination of mitral regurgitation. *Echocardiography* 1990;7(6):747–62.
- [8] Oppenheim A, Schaffer R, Buck J. *Discrete-time Signal Processing*. Englewood Cliffs, New Jersey: Prentice Hall, 1999.
- [9] D'Hooge J, Heimdal A, Jamal F, Kukulski T, Bijnens B, Rademakers F, Hatle L, Suetens P, Sutherland GR. Regional strain and strain rate measurements by cardiac ultrasound: principles, implementation and limitations. *Eur J Echocardiogr* 2000;1(3):154–70.
- [10] Bermejo J, Antoranz J, Yotti R, Moreno M, García-Fernández M. Spatio-temporal mapping of intracardiac pressure gradients. a solution to Euler's equation from digital postprocessing of color doppler m-mode echocardiograms. *Ultrasound in Med Biol* 2001;27(5):621–630.
- [11] Greenberg NL, Vandervoort PM, Thomas JD. Instantaneous diastolic transmitral pressure differences from color doppler m mode echocardiography. *Am J Physiol* 1996;271(4 Pt 2):H1267–76.

Address for correspondence:

José Luis Rojo-Álvarez
4.3.B.2, Av Universidad 30, Universidad Carlos III de Madrid
28911, Leganés, Madrid (Spain)
E-mail to: jlrojo@tsc.uc3m.es